Contrasting spin-polarization regimes in Co nanowires studied by density functional theory

Ben Hope*
Nanoscience Centre, Department of Engineering, University of Cambridge, 11 J.J. Thomson Avenue, Cambridge CB3 0FF, United Kingdom

Andrew Horsfield†
Department of Materials, Imperial College London, South Kensington Campus, London SW7 2AZ, United Kingdom
(Received 29 September 2006; revised manuscript received 7 October 2007; published 31 March 2008)

In electronic structure calculations of magnetic nanostructures, a commonly used definition of the degree of spin polarization (DSP) employs only the density of states (DOS) at the Fermi level. However, the Fermi velocity can also play a crucial role in the DSP in ballistic and diffusive transports. We illustrate this by investigating the spin-dependent electronic structure of freestanding cylindrical hcp Co nanowires with diameters of up to 11.6 Å. Using density functional theory, the energy bands and DOS are calculated. For all but the monowire, we find that there is stark disagreement between the DOS, ballistic, and diffusive DSPs: they are highly negative, small, and highly positive, respectively. This is shown to result from the nature of *d* and *s* bands together with hybridization effects and bond formation.

DOI: 10.1103/PhysRevB.77.094442 PACS number(s): 75.75.+a, 73.22.−f, 72.25.−b, 71.15.Mb

I. INTRODUCTION

Spintronics is an exciting area in nanoscience.[1–4] Its aim is to transport, manipulate, and store information by utilizing the spin degree of freedom of charge carriers. Perhaps the most exotic prospect is quantum computation[5] which relies on the coherent evolution of individual entangled qubits to perform fundamentally new operations. However, the use of spin (instead of, or in combination with, charge) is also likely to have a major impact on the implementation of classical algorithms. When advances in conventional silicon processor technologies start to hit elementary physical limits,[6] further significant improvements in performance could still be achieved by encoding information in the average spin of an ensemble of particles. Being governed by the time-reversible Schrödinger equation, spin rotation is a thermodynamically reversible process. Therefore, using spin states to process information is one route to nondissipative computation which could permit chip densities that are otherwise inaccessible due to heating malfunctions. Radical "chameleon" spintronic processors have even been conceived [7,8] which could, in principle, be reconfigured in nanoseconds to perform the logical functions optimal for a given calculation and thus yield further dramatic increases in computational speed. Other important possible payoffs are increased memory capacity[9] and the nonvolatility of output, a property already employed in magnetic random access memory devices.

The success of these efforts requires the theoretical and practical resolution of several technical problems. One primary issue is that of generating and detecting currents of highly spin-polarized electrons.

If a net current I exists in a system, then its degree of spin polarization (DSP) P_I is given by the generic definition

$$P_I = \frac{I_\uparrow - I_\downarrow}{I_\uparrow + I_\downarrow}, \tag{1}$$

where $I_{\uparrow(\downarrow)}$ is the current of spin-up (down) electrons. $I_{\uparrow(\downarrow)}$ are not directly measurable, but several effects are observed, which imply the existence of a nonzero DSP whose value can be either directly measured or inferred.[10] One of the most important such effects is spin-dependent tunneling. Notable studies of this were first presented by Tedrow and Meservey[11–13] whose discoveries were an antecedent of the groundbreaking observations of tunneling magnetoresistance (TMR) in magnetic tunnel junctions made by Julliere[14] in 1975. Other important phenomena revealing a DSP include spin-polarized photoemission[15] and the Andreev reflection.[16] These experiments buy their spintronic functionality through a probing of the spin-dependent (Fermi-level) electronic structure of the constituent materials. This often entails relating the polarization to the measured quantities through a theoretical model that employs the relevant features of the electronic structure. Several expressions for the DSP arise in such models; in this paper, we illustrate three key examples.

The arrival of these observations, along with remarkable recent advances in fabrication techniques, has ignited an explosion in theoretical papers presenting electronic structure calculations with the aim of characterizing nanostructures for use in spintronics: a high DSP in the electronic structure automatically endows the system with some spintronic potential. Many are concerned with quasi-one-dimensional systems involving transition metals[17–31] (TMs) which are likely to play a central role in the quest for spin-polarized currents because of their large exchange energies. In this endeavor, perhaps the most commonly cited expression for the DSP is the so-called "N" or "density of states (DOS)," definition given by

$$P_N = \frac{N_\uparrow(E_F) - N_\downarrow(E_F)}{N_\uparrow(E_F) + N_\downarrow(E_F)}, \tag{2}$$

where $N_{\uparrow(\downarrow)}(E_F)$ denotes the density of spin-up (down) states at the Fermi energy E_F. This equation is obtained from a classical Drude model of conduction[32] and provides a measure of the relative number of carriers available for each spin. It also appears in—or is usually assumed to be the DSP

appearing in—Julliere's elegant and very often successful model of TMR,[14] which may explain its prevalence.

However, the relevance of Eq. (2) to Eq. (1) is limited by the fact that it is obtained entirely from the DOS at the Fermi level, when in reality, Fermi group velocities can also play an important role in electronic conduction. Indeed, as Mazin[33] first pointed out in the context of the Andreev reflection, the extent to which the Fermi velocities affect P_I depends crucially on the type of conduction present in the experiment, which is itself largely determined by the physical length scales of the system. In particular, he highlighted the distinction between ballistic and diffusive transports.

The ballistic conduction regime is that in which the phase coherence length l_ϕ and mean free path L_m are both much longer than the size of the specimen L. In this limit, the formalism of Landauer and co-workers[34–36] can be applied to show that the conductance, or equivalently current, associated with a Bloch state k is proportional to the product $N_k v_k$ of its Fermi-level DOS and group velocity. Since the electron velocity and DOS are inversely proportional, they cancel each other and the total spin-up (down) conductance is just a constant multiple of the number $X_{\uparrow(\downarrow)}$ of spin-up (down) bands crossing the Fermi level in the direction of the transport. This yields the Nv definition of spin polarization applicable in the ballistic regime,

$$P_{Nv} = \frac{\langle N_\uparrow|v_\uparrow|\rangle - \langle N_\downarrow|v_\downarrow|\rangle}{\langle N_\uparrow|v_\uparrow|\rangle + \langle N_\downarrow|v_\downarrow|\rangle} = \frac{X_\uparrow - X_\downarrow}{X_\uparrow + X_\downarrow}, \tag{3}$$

where $\langle N_i|v_i|\rangle$ $(i=\uparrow\downarrow)$ is the integral of $N_i|v_i|$ over the Fermi energy.[72]

The diffusive regime is characterized by a phase coherence length that is considerably longer than the mean free path so that (elastic) scattering becomes important and quantum interference effects are averaged out. In general, l_ϕ is also considered shorter than L, but this is not the important point. Transport in this limit is described by the classical Boltzmann theory.[37] Assuming spin-independent relaxation times, the current is now proportional to the product $N_k v_k^2$ and the overall conductance is obtained by integrating this over the Fermi energy. Again, one power of the velocity cancels with the density of states and thus the result is proportional to the sum of the gradients of the Fermi-level band crossings. Hence, the Nv^2 spin polarization, which applies in the diffusive regime, is given by

$$P_{Nv^2} = \frac{\langle N_\uparrow v_\uparrow^2\rangle - \langle N_\downarrow v_\downarrow^2\rangle}{\langle N_\uparrow v_\uparrow^2\rangle + \langle N_\downarrow v_\downarrow^2\rangle} = \frac{\Sigma_\alpha v_{\uparrow\alpha}(E_F) - \Sigma_\beta v_{\downarrow\beta}(E_F)}{\Sigma_\alpha v_{\uparrow\alpha}(E_F) + \Sigma_\beta v_{\downarrow\beta}(E_F)}, \tag{4}$$

where α (β) is a band index running over the up (down) bands that cross the Fermi level.

The Nv and Nv^2 definitions are often not considered. For example, Yang *et al.*[17] and Kang *et al.*[28] simulated nanowires of Co and Fe, respectively, both in the freestanding state and encased in single-walled carbon nanotubes. It is found that these structures exhibit a high degree of spin polarization as defined by Eq. (2), but no mention is made of any other DSP. Since the three polarizations can assume wildly different values in a single crystal, this may lead to an incomplete picture. Moreover, given the important techniques, such as the point contact Andreev reflection spectroscopy,[38–42] for which P_{Nv} and P_{Nv^2} are the appropriate scales, such omissions could limit the range of applications to which the results can be applied.

It should be noted that the expressions given above are not comprehensive; even the DSP definitions that incorporate Fermi velocity have their limitations in specific experimental scenarios and further expressions have been developed as a result. In the diffusive regime, for example, if the scattering rates are spin dependent, or spin-flipping mechanisms are present, the expression for the DSP [Eq. (4)] becomes more complicated[33] with the possibility of another spin-projected DOS factor.[43] This emphasizes the need to be careful about the nature of the scattering in the system under consideration. Furthermore, in tunneling experiments, the physical and electronic structure of the barrier and the nature of the bonding at the interfaces can be important. Indeed, as Soulen *et al.*[44] noted, the results of Tedrow and Meservey are more accurately described by incorporating tunneling matrix elements into the DSP equation. These are determined by the overlap of wave functions at the interface and are, in general, spin dependent. The same factors, along with exchange-induced wave-vector discrepancies between states on either side of the barrier, also place limits on the success and validity of the Julliere model, as highlighted by more sophisticated theoretical approaches to the phenomenon.[45–49] Further complications can arise when dealing with additional parameters such as temperature.[50] Despite these qualifications, a wide range of behavior can be demonstrated using the models most often considered; specific cases may require additional models, but compared to P_N alone, the three main definitions given above provide a much clearer picture of the spin dependence of an electronic structure, and one that is sufficient for our purposes.

That Eqs. (2)–(4) are not necessarily correlated in a simple way becomes clear when we consider the effect of varying the DOS, velocities, and number of crossings at the Fermi energy. Recall that group velocities are directly and inversely proportional to band gradients and DOS, respectively. In the limit in which gradients are identical at all crossings, the three expressions all agree. Therefore spin-dependent Fermi velocities are necessary for differing DSPs—discrepancies in the number of crossings only act to amplify or suppress differences created by the slopes. When the spin-projected Fermi velocities do differ, a range of results is possible. The qualitatively distinct cases, under the assumption of the constant Fermi velocity for each spin, are summarized in Table I. If velocity is allowed to vary within spins, then there are even more cases. Note that if the spin dependence is large enough, there could even be sign changes in going from P_N to P_{Nv^2}. The key point is that the relative weight of the DOS and the velocity is different in each definition, and this will reflect spin-dependent Fermi gradients.

A special class of material for which all three DSP definitions concur is the half-metal (HM). These are characterized by a nonzero number of crossings for one carrier and zero for the other. The corresponding DOS vanishes in a gap around the Fermi energy for one spin only, and the result is 100% spin polarization in all regimes. While this is the case

TABLE I. The effect on P_N, P_{Nv}, and P_{Nv^2} of varying the number of Fermi-level crossings $X(E_F)$ and the Fermi velocity v_F for each spin. These are the distinct cases, up to an overall change in sign, assuming Fermi velocity is roughly constant for each spin. There are more cases if velocity is allowed to vary for individual spins. "−" indicates the sign of the DSP is negative while "low" could be either sign. "Depends" means that any value is possible with some specific example. Cases 1 and 5 are the most important for this paper. In case 1, there is a large discrepancy in the number of spin-up and spin-down bands yet similar slopes throughout which gives a high P_{Nv} and a high P_N. In case 5, the numbers of spin-up and spin-down bands roughly equate and yet a large difference in their gradients at E_F, in favor of spin up, results in a large negative P_N and a vanishing P_{Nv}.

	$X(E_F)$		v_F				
	$X_\uparrow$	$X_\downarrow$	$\uparrow$	$\downarrow$	P_N	P_{Nv}	P_{Nv^2}
1	Small	Large	Roughly equal		−High	−High	Moderate changes possible but sign change unlikely
2			Small	Large	Depends	−High	−High
3			Large	Small	−Very High	−High	Possibly big differences including sign change
4	Roughly equal		Roughly equal		Low	Low	Low
5			Large	Small	−High	Low	Possibly big differences including sign change

for a perfect HM, from the above discussion, it is conceivable that a structure might *approximate* to a HM—with a very high DSP—in one conduction regime, but reach nowhere near it in others. We give an example of such a structure later.

The conduction bands of magnetic transition metal nanowires comprise both high-speed low-density *s* electrons and low-speed high-density *d* electrons. This makes them ideal candidates not only for investigating high polarization for spintronic applications but also for illustrating the different DSPs. In Sec. III, we present the results of a systematic study of the spin-dependent electronic structure of freestanding cylindrical hcp Co nanowires, in the ferromagnetic state, up to a diameter of 11.6 Å (14.3 Å if atomic radii are included). With the exception of the monatomic wire (monowire), we do indeed find a notable disagreement between the DSP expressions. The DOS and diffusive DSPs are large in magnitude and opposite in sign, while the ballistic DSP is small. The underlying reasons are discussed in detail, including the effects of hybridization and bonding. Computational details are given in Sec. II B.

II. MODEL

A. Nanowire structures

Apart from the monatomic chain, the nanowires considered in this paper are formed by cutting cylinders from hcp cobalt. Taking an atom at the origin and the wire axis in the z direction, coincident with the [001] axis of Co, we increase the cylinder diameter up to 11.6 Å to encompass increasing numbers of atoms. This yields a total of eight distinct unit cells, each with threefold rotational symmetry about the z axis. These are illustrated in Fig. 1 along with the monowire. The cells consist of two (001) planes—plane A and plane B—containing Co atoms arranged at each point of a triangular Bravais lattice with the two layers offset such that they get stacked in an ABABAB$\cdots$ configuration along the z axis. The cell dimensions are taken from Ref. 51: the cell length [one dimensional (1D) lattice constant] is c=4.070 Å with plane B a perpendicular distance $c/2$ from plane A and, prior to relaxation, the Co-Co nearest neighbor distance is 2.507 Å. We adopt the notation Co_n to denote the Co wire with n atoms in the unit cell.

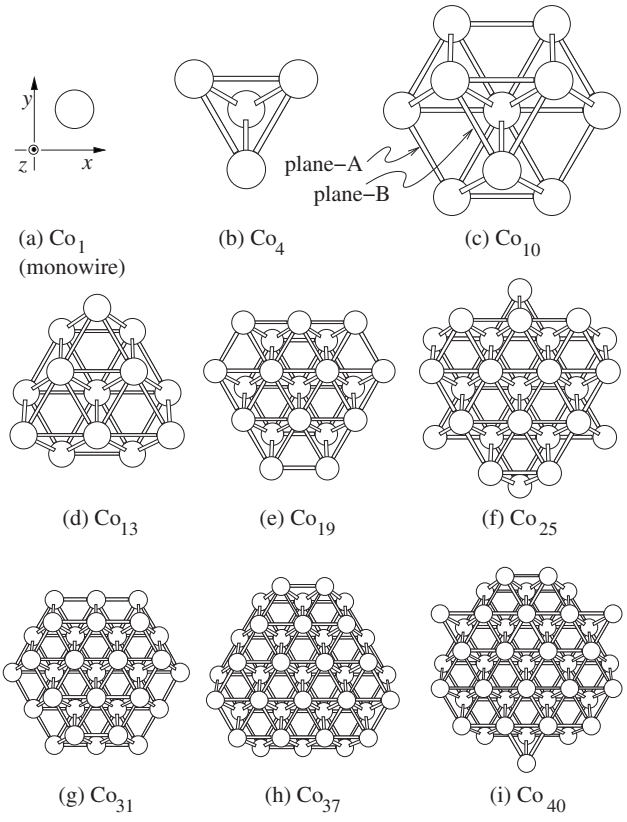

FIG. 1. Unit cells of Co nanowires. (a) The monatomic chain which has a relaxed lattice constant of 2.17 Å. [(b)–(i)] The polyatomic wires which are cut from hcp Co with the axis in the z direction (out of the paper) coincident with the [001] axis of Co. Each cell consists of two planes of atoms (planes A and B), separated by a perpendicular distance $c/2$, where c is the length of the lattice vector. We take c=4.070 Å and, prior to relaxation, the Co-Co nearest neighbor distance is 2.507 Å. A wire with n atoms in the unit cell is denoted Co_n.

For the calculations outlined below, each nanowire unit cell from Fig. 1 is placed into an otherwise empty supercell to which periodic boundary conditions are applied. This creates an infinite array of nanowires, but the supercell is made large enough to leave a vacuum radius of 6.0 Å around each which prevents any unwanted interactions between neighboring wires.

B. Computational details

All our calculations have been implemented by the Vienna *ab initio* simulation package (VASP) using the projector augmented wave method and generalized gradient approximation of density functional theory. The plane-wave basis set used had a cutoff energy of 348.36 eV. The Gaussian smearing was employed with a width of 0.05 eV, and the self-consistent iterations were allowed to converge to within 10^{-5} eV.

A Γ-centered k-point mesh was used throughout, and energy-convergence tests were done to decide on an appropriate axial mesh density n_k for sampling the first Brillouin zone. A mesh density of 30 k points was found to be sufficient. Since the three DSPs were calculated [using Eqs. (2)–(4)] from the DOS and energy bands produced by VASP, we also checked the convergence of the Fermi velocities and DOS. Using Co_1 and Co_4 as test cases, these properties were remarkably insensitive to k-point density: between $n_k=10$ and $n_k=60$, the resulting DSPs did not vary by more than a single percentage point.

For the polyatomic ($n>1$, polywire) simulations, the atoms were allowed to relax inside the cell with an energy-convergence threshold of 10^{-4} eV. In doing this, the supercell dimensions were fixed, but we did compute total energy as a function of cell length for Co_4, with the A-B interlayer distance held *constant* at 2.03 Å. This confirmed that the atoms are stable against clustering. For the monatomic chain, Co_1, we relaxed the structure by minimizing the energy with respect to the lattice constant. This gave a bond length of 2.17 Å, in good agreement with previous authors.[22,52,53]

Throughout, only ferromagnetic input configurations were considered with all initial magnetic moments set at $4.0\mu_B$. The spin-orbit and dipole-dipole interactions were both neglected.

III. RESULTS

For the polywire cells, the ionic relaxation process results in some movement of the atoms, but it is minor; essentially, the wires constrict a little while the symmetries remain largely unbroken. Typically, the outer atoms undergo a displacement toward the core of about 0.17 Å. The outermost atoms of Co_{25} and Co_{40} move a little further inward (with displacements of 0.25 and 0.29 Å, respectively) because they lack the bonds—they have coordination number, $z=4$—to hold them in position from many directions. Moreover, there is more charge available, per bond, to fill the bonding states and provide a stronger hold toward the wire axis. The atoms closer to the core move a lot less and there is no movement parallel to the axis.

Figure 2 shows the d- and sp-projected DOSs for the (relaxed) freestanding ferromagnetic Co nanowires and also for bulk hcp Co. Each figure has the familiar transition metal feature of narrow d bands superimposed onto wide free-electron-like sp bands.[54] With increasing n, the DOS becomes more bulklike. In all cases, significant magnetization is apparent: the spin-projected densities of states are offset such that a much greater proportion of one set of states, relative to the other, is left unoccupied above the Fermi energy. The majority and minority spin electrons are those whose spin is, respectively, parallel and antiparallel to the magnetization of the material; we take the majority to be spin up.

The d bands are almost fully occupied for the majority electrons leaving a very small density at the Fermi energy. In contrast, for the minority spins, the Fermi energy is located where the DOS is still high. Thus, the exchange splitting of the d bands is also responsible for a large negative P_N in all structures. The density is, however, nonzero for majority spin states at the Fermi level, and furthermore some of these conduction electrons are in the sp bands. It is at this point that the DOS alone does not provide sufficient information since, although they do not contribute much to the density, these carriers move fast and so have important implications for the polarizability of ballistic and diffusive currents. To quantify this, Table II shows P_{Nv} and P_{Nv^2}, calculated from the band structures corresponding to the densities of states of Fig. 2, along with the figures for P_N obtained directly from the DOS. The DOS DSP for bulk hcp Co and the crossing counts X, used to obtain P_{Nv}, are also included. Figure 3 offers a graphic illustration of these results with each DSP plotted against the number of atoms in the cell.

A. Degree of spin polarization in the monowire

It is clear that, with all three DSPs agreeing in sign, the monochain is something of an exception. To elucidate this, we examine its band structure around the Fermi energy which is shown in Fig. 4(b). From the five d orbitals on each atom, just three types of bond may be formed, which preserve angular momentum about the bond axis.[54] These are depicted in Fig. 4(a) and are labeled $dd\sigma$, $dd\pi$, and $dd\delta$ because they are formed from orbitals which have angular momentum z components m of 0, ±1, and ±2, respectively. By projecting the band structure onto these orbitals, it is possible to identify which bands they generate. The results are given by the band labels in Fig. 4(b). The magnitude of the hopping integrals grows as the overlap between the atomic orbitals increases. Looking at the bonds [Figure 4(a)], the lobes in $dd\sigma$ overlap the most and the lobes in $dd\delta$ overlap the least. It is therefore consistent that we find the $dd\sigma$ band to be the widest (fastest) and the $dd\delta$ band to be the narrowest (slowest). As indicated, there is some hybridization with the sp-dominated band. While this has little qualitative impact for the monowire, we will see that the effect is more significant in the polyatomic wires.

The exchange splitting causes a highly spin-dependent conduction channel count of six to one in favor of the minority carriers (the $dd\pi$ and $dd\delta$ bands are doubly degener-

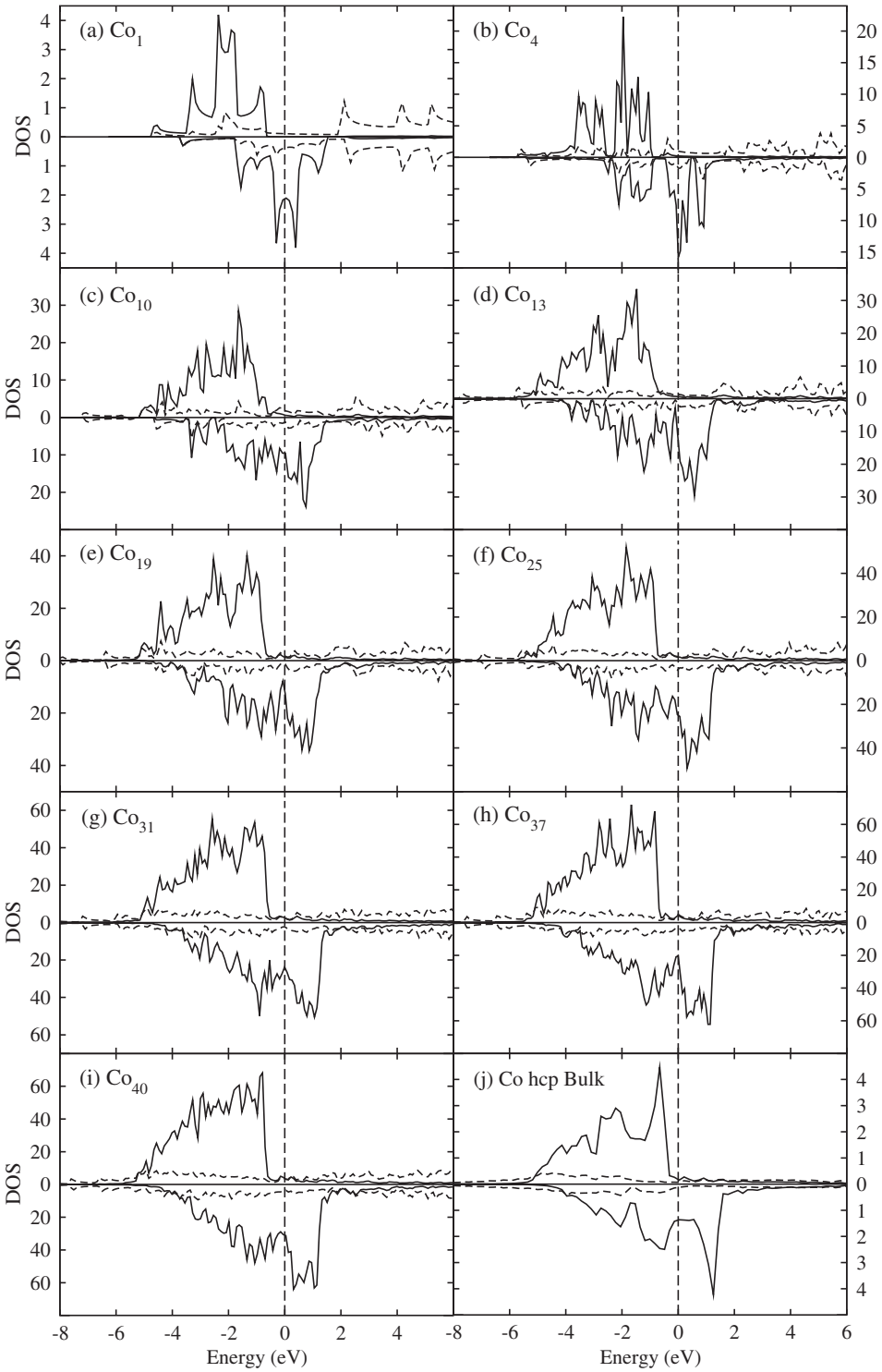

FIG. 2. The DOS projected onto the *d* (solid line) and *sp* (dashed line) orbitals for [(a)–(i)] the freestanding ferromagnetic hcp Co nanowires and (j) bulk hcp Co. The top (bottom) panel in each represents the majority (minority) spin. The vertical dashed lines run through the Fermi energy which is set to zero.

ate). We essentially have case 1 from Table I: there is a large difference in the number of bands at E_F but an ineffective spin dependence in the Fermi velocity. The single *sp*-like majority band is balanced by a corresponding minority one leaving the rest of the minority bands free to influence the DSPs. It is this difference in crossing number, rather than extreme differences in Fermi velocity, that gives the monochain its characteristic polarization properties. It has, in magnitude, the largest N DSP of −92%, it is the only one of the structures to have a considerable ballistic DSP at −71%, and its single spin-up term in Eq. (4) has little impact so that the diffusive DSP is also negative. Hence, all three DSP expressions agree in sign and the only thing preventing half metalicity is the single *sp* majority crossing.

Monatomic Co nanowires have been investigated several times already both theoretically[22,30,52,53,55–57] and experimentally.[58–61] Nautiyal *et al.*[22] provided an exception to the consensus by claiming complete spin polarization,

TABLE II. The degree of spin polarization (DSP) in freestanding ferromagnetic hcp Co nanowires. The DOS (P_N), ballistic (P_{Nv}), and diffusive (P_{Nv^2}) DSPs are calculated using Eqs. (2)–(4), respectively. All DSPs are quoted in % and are allowed, by definition, to assume negative values. $X_{\uparrow(\downarrow)}$ denotes the number of spin-up (down) bands crossing the Fermi energy, used to compute P_{Nv}, and X_{tot} is the sum of these to give the total number of conduction channels.

	X					
Structure	X_{tot}	$X_{\uparrow}$	$X_{\downarrow}$	P_N	P_{Nv}	P_{Nv^2}
Co_1	7	1	6	−92	−71	−43
Co_4	6	3	3	−87	0	95
Co_{10}	7	4	3	−62	14	47
Co_{13}	12	6	6	−76	0	74
Co_{19}	13	6	7	−61	−8	48
Co_{25}	18	9	9	−78	0	64
Co_{31}	20	11	9	−67	10	80
Co_{37}	25	14	11	−43	12	56
Co_{40}	29	15	14	−65	3	67
Bulk	–	–	–	−72	–	–

with only minority carriers available for conduction. There is otherwise broad agreement throughout the literature and our results largely concur.

B. Degree of spin polarization in the polywires

In stark contrast to the monowire, all the polywires reveal strong disagreement between the DSP expressions. Referring to Fig. 3, the ballistic DSP, P_{Nv}, is small for all $n>1$, oscillating about zero as n increases. In contrast, the DOS and diffusive DSPs are large in magnitude and opposite in sign,

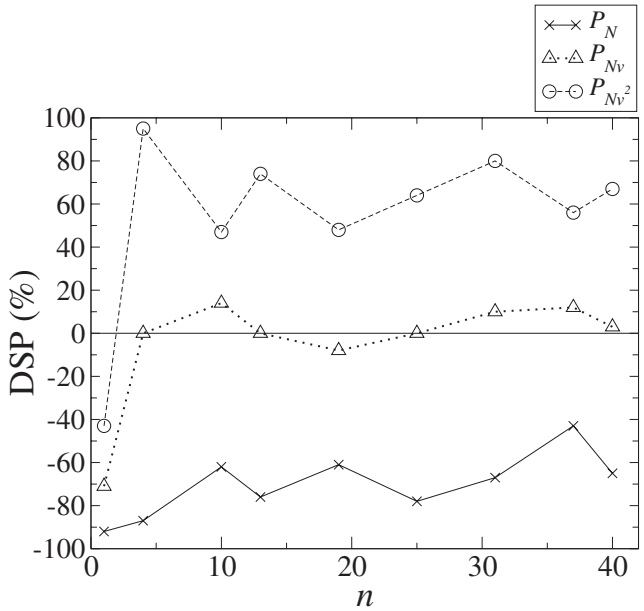

FIG. 3. The DSP in freestanding ferromagnetic hcp Co nanowires as a function of the number n of atoms in the unit cell. Crosses, triangles, and circles denote the DOS (P_N), ballistic (P_{Nv}), and diffusive (P_{Nv^2}) spin polarizations, respectively.

with P_N negative and P_{Nv^2} positive. Their slight oscillatory variation with n is synchronized so that they appear as approximate mirror images about the zero line. This is a direct consequence of the inverse weighting of velocity in their respective definitions, combined with the similarity between the two spins, in the number of bands crossing E_F.

The polyatomic wires are examples of case 5 from Table I with the number of majority and minority crossings roughly equal and yet a considerable difference in gradient at the Fermi energy consistently favoring the majority carriers. This is observable in the spin-resolved band structures which, for Co_4 and Co_{10}, are shown in Figs. 5(a) and 5(b), respectively. Note how shallow the minority d conduction bands are (right panels) compared with the majority bands (left panels) which projection confirms are predominantly sp. To illustrate this further, Figs. 5(c) and 5(d) depict the corresponding electron charge-density distributions, on slices through the unit cells at a distance half way between the two layers, for electrons with energy near the Fermi level. The spin-up density (left panels) shows considerable delocalization, in contrast to the relative constriction of the spin-down d orbitals (right panels), a pattern repeated at all slice positions throughout the unit cells of the polywires. Compared with the sp states, the highly localized d orbitals do not overlap very much with the orbitals on neighboring atoms and hence hopping integrals between these d orbitals are relatively small. This is consistent with the intuitive picture of a few "light" or fast-traveling spin-up electrons balancing large quantities of "heavy" or slow spin-down electrons to produce equal currents in the ballistic limit. Nadgorny *et al.*[38] and Panguluri *et al.*[42] obtained similar results for systems of Ni_xFe_{1-x} and Mn_5Ge_3, respectively.

C. Why the difference?

It remains to explain why the band structure at the Fermi energy has this character for all $n>1$. In particular, we need

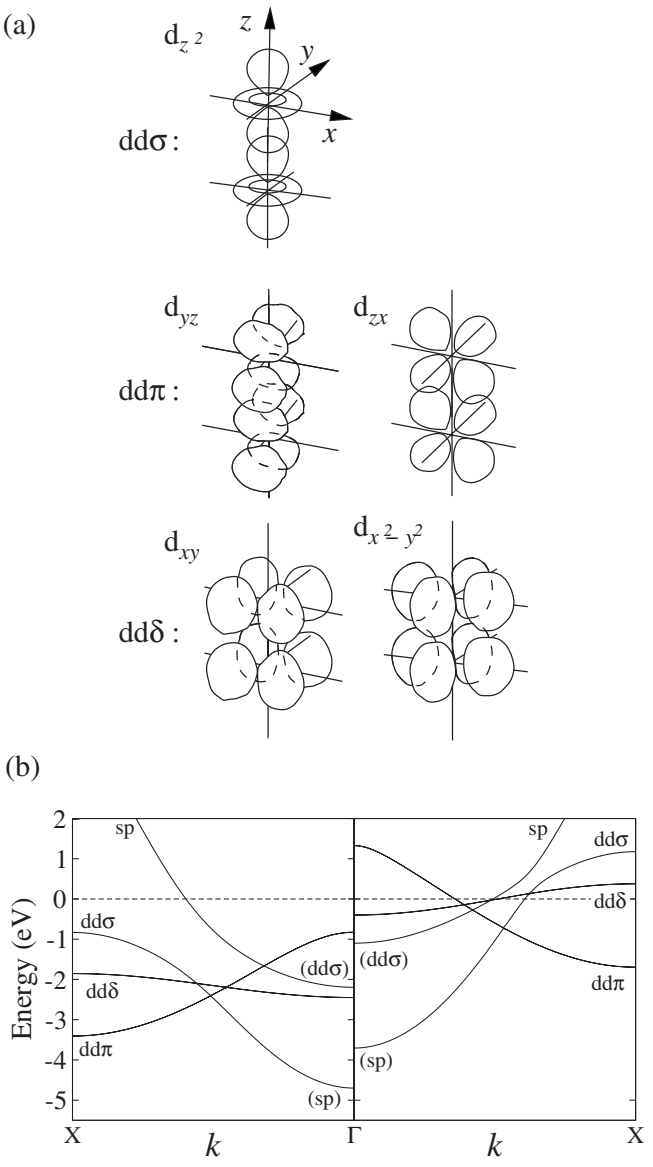

FIG. 4. (a) The three fundamental hopping integrals between *d* states on neighboring atoms and the orbitals from which they are formed. (b) The energy-band structure of the freestanding Co monatomic chain with the majority and minority spins shown in the left and right panels, respectively (as opposite halves of the first Brillouin zone). The labels denote the dominant bond with those in brackets (on the left) indicating some significant contribution from that bond, in that area, owing to hybridization. The $dd\pi$ and $dd\delta$ bands are doubly degenerate in accordance with the bonds displayed in (a). The dashed line represents the Fermi level which is set to zero.

to know why there is such a sharp reduction in the ratio of minority to majority crossings, why the *sp* crossings are not vastly outnumbered by the *d* channels, as they are in the monochain, and why there are not roughly equal numbers of up and down *sp*-dominated bands given that exchange splitting is much less effective for such states. To answer these questions, we need to explore two effects.

The first is a suppression of the increase in minority *d* crossings as *n* increases. We might expect the number of minority *d*-dominated bands crossing the Fermi energy to be directly proportional to *n*, but this is not the case. As shown in column 4 of Table II, there is instead a decrease in going from Co_1 to Co_4, followed by a gradual and sporadic increase with *n*. Of course, $X_\downarrow$ is the total number of minority bands, so it could include *sp*-dominated bands or at least bands with a significant *sp* contribution. As it happens, $X_\downarrow$ does not involve any such contributions but even if it did, it would only *reinforce* this point.

This suppression in the increase of minority *d* crossings results from *lateral bond formation*, which is the creation of bonds with, and between, off-axis atoms, which occurs as soon as $n>1$. In the monowire, there are no off-axis atoms; the bonds are all lined up along the axis so that the electrons can hop easily down the chain. Bonding and antibonding states exist, but they are within individual bands which cross the Fermi level. The polyatomic wires are, by comparison, more akin to a series of clusters. Atoms are no longer aligned along the *z* direction in such close proximity and bond axes point in a larger variety of directions. Complete sets of minority channels become fully occupied bonding bands below the Fermi energy, in effect removing conduction electrons for use in structural stability. The bonding and antibonding states now form separate peaks as is discernible in the DOS for some $n\neq 1$ [Fig. 2, especially (b) Co_4].

The effect is also seen graduated in the DOS projected onto individual atoms in a wire. Figure 6, for example, depicts the *d* PDOS for the three distinct atomic classes of nanowire Co_{10}. Solid, dashed, and dotted lines represent projections onto the core, intermediate, and outermost atoms, respectively. There is an increase in separation between the bonding and antibonding peaks in going from outlying to central atoms, in conjunction with an increase in coordination number and therefore off-axial hybridization of *d* orbitals. Kang *et al.*[28] also highlighted this effect. The same topological changes occur for the majority bands, but being almost fully occupied with little weight at the Fermi energy, this is not relevant to the present question.

Thus, while inevitably there are more minority *d* conduction channels open for larger *n*, there are fewer than we would expect from an equivalent number of independent monowires. The biggest increases in $X_\downarrow$ occur in forming Co_{13} and Co_{40}, the two occasions on which just three Co atoms are added at the periphery of the previous cell. These atoms have low coordination number, so it is similar to adding independent chains.

The second effect is the apparent expulsion of *sp* bands from the *d*-dominated regions, which results from *sp-d hybridization*. Figure 7 shows the minority band structure for Co_{10} near the Fermi energy. Points are marked by circles, the size of which is proportional to the contribution from *d* states and *sp* states in the left and right panels, respectively. The hybridization of *d* and *sp* bands here causes states that would otherwise be *sp*-like to assume a *d* character when close in energy to the *d* bands. Consequently, the *sp* bands appear as being deflected away from the *d*-dominated region. The same occurs for the majority bands, but it does not affect $X_\uparrow(E_F)$ to the same extent because the majority *d*-dominated region is

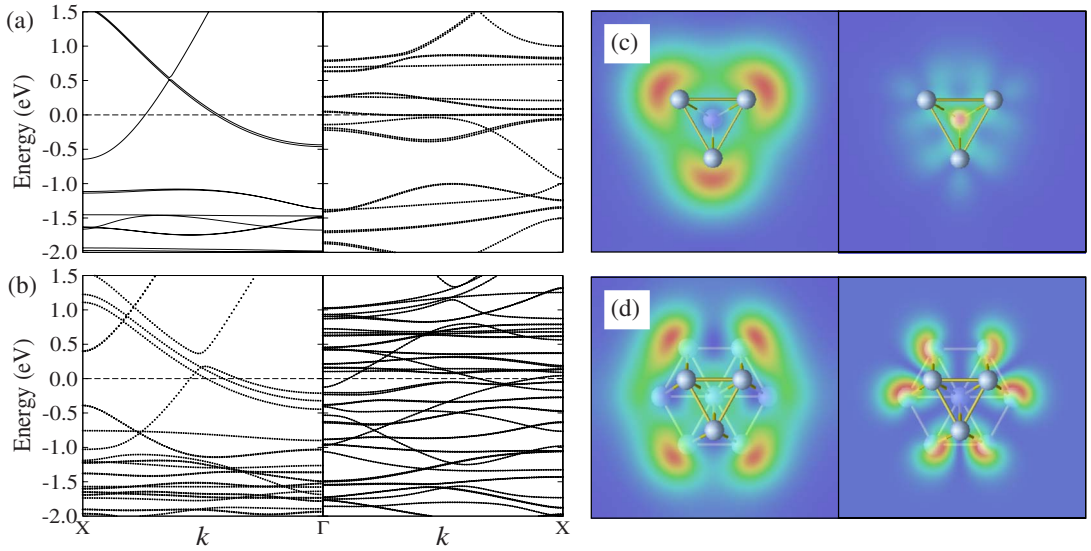

FIG. 5. (Color online) The energy-band structures of nanowires (a) Co_4 and (b) Co_{10}. With k in opposite halves of the first Brillouin zone, the majority and minority spins are shown in the left and right panels, respectively. The Fermi energy is set to zero. (c) and (d), respectively, show the corresponding charge-density distributions, on slices through the unit cells, for electrons whose energy lies within 0.03 eV of the Fermi level. The slices lie in the x-y plane, midway between the two layers of atoms in the unit cell. The left (right) panels show the majority (minority) spin.

centered away from the Fermi energy. Thus, the *sp* bands are excluded from the Fermi level for the minority spin only. It is this effect, rather than the insignificant *sp* exchange splitting, which results in Fermi-level polarization of the *sp* states.

The two effects described above give the underlying reasons why P_{Nv} becomes very small: suppression of the increase in minority *d* crossings and effective expulsion of minority *sp* bands from the Fermi region result in numbers of up and down bands at the Fermi energy that approximately equate. Furthermore, the effect of *sp*-*d* hybridization at the Fermi energy shows why the wide majority *sp* bands are not balanced by corresponding fast minority bands, which leads to a large and positive P_{Nv^2}.

D. Discussion

Perhaps the most remarkable of the structures is Co_4. With 95% polarization in the diffusive regime, it holds the highest DSP across all definitions and all wires and yet it attains zero spin polarization in the ballistic regime. It thus exemplifies the structures, envisioned in Sec. I, which closely approximate to a HM in one limit but behave as exact opposite of the other. In principle, therefore, a complete switch in behavior, from spin-blind transport to *nearly* HM, could be achieved in such systems simply by inducing a change in the type of conduction present, the most obvious method for which being a change in length.

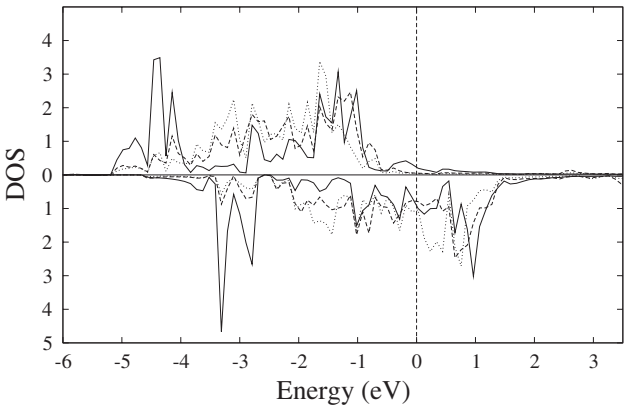

FIG. 6. The projected densities of states for *d* orbitals on the three distinct atom classes of nanowire Co_{10}. Solid, dashed, and dotted lines denote the projections onto the core, intermediate, and outermost atoms, respectively. The vertical dashed line runs through the Fermi energy which is set to zero.

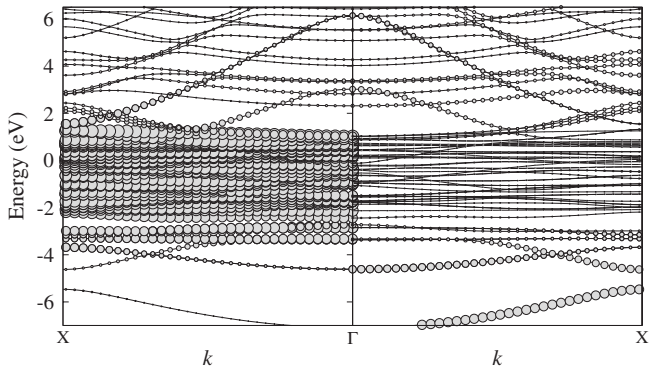

FIG. 7. The minority band structure for nanowire Co_{10}. The left and right panels show opposite halves of the first Brillouin zone in which the size of each circular symbol is proportional to the contribution from *d* and *sp* states, respectively. The Fermi energy is set to zero and the data-point density has been reduced for clarity.

Co_4 is also notable for the gap in the minority DOS which occurs above the Fermi energy at approximately 0.5 eV. This is visible in both Figs. 2(b) and 5(a). If the Fermi energy was somehow made to match this value, then Co_4 would behave as a HM, with perfect spin polarization, because the spin-down conductance would vanish. A similar gap occurs at about 0.7 eV *below* E_F for the majority spin, and it is again unmatched since there is a single minority band through this window [see Fig. 5(a)]. However, unlike some nanostructures investigated by other authors[19,24,27,62] which exhibit unambiguous gaps for one carrier at the *Fermi energy*, our calculations do not predict any genuine half-metalicity. The best the Co_n can offer alone is an approximation to half-metalicity under particular definitions. Sabirianov *et al.*[30] came to similar conclusions on this issue for fcc Co nanowires of square cross section.

Given that the type of conduction in operation depends on the sample length, it has nothing to do with, or cannot be deduced from, the energy-band structure—they are separate issues. It is therefore proper procedure to calculate all three DSPs and then address the question of what to expect given samples of different lengths. Yet, there may be a legitimate concern over the characteristic transport lengths of transition metals. For example, if the Co nanowires do not behave ballistically, then observations concerning P_{Nv} become irrelevant. In magnetic transition metal structures, Ref. 63 gives a mean free path and phase coherence length of 10–20 Å and 100–200 Å, respectively. If the Co nanowires exhibit such values, then they are indeed not very conducive to ballistic transport. However, given a device short enough, all conducting materials can be made to satisfy the ballistic condition. For the Co monowire and polywires, this implies a ration of less than nine and five unit cells, respectively. Whether or not Co components of this length are likely to feature strongly in spin-transport designs remains to be seen, although TM nanocontacts are already the subject of much research.[64,65] Moreover, there are additional complications for such systems because calculations based on wires that are effectively infinite in length lose some applicability as the energy bands start to resemble discrete energy levels instead. Thus, we may be reduced to the qualified statement: for segments of Co nanowire short enough to support ballistic conduction, and to the extent that our results are then relevant, the universally low P_{Nv} scores—monowire excepted—suggest that severe limits are placed on their use in spin-polarized transport. This only affects devices and components relying on properties of the ballistic regime. Applications designed to employ a high diffusive DSP, or which rely only on a large polarization in the Fermi-level DOS, are untouched.

The spin-orbit interaction plays an important role in several nanoscale effects. For example, through magnetocrystalline anisotropy, there is considerable evidence to suggest that it prevents superparamagnetism—in Co monowires, in particular—by stabilizing the long-range order which can become more susceptible to thermal disruption in conditions of reduced dimensionality.[55,58,60] This has important implications for high-density information-storage applications, and given that a high Fermi-level DSP is a by-product of the ferromagnetic state, magnetocrystalline anisotropy can, in addition, be seen as supporting an electronic structure suitable for spin-polarized transport. The omission of spin orbit from theoretical accounts of these effects is clearly a serious flaw.

In the present case, there is the possibility of spin orbit affecting the band structures at the Fermi energy—the number of crossings, the slopes, or both—in a way which would change the DSP scores. With relevance to this and effects such as ballistic anisotropic magnetoresistance, Mokrousov *et al.*,[29,66] Velev *et al.*,[67] and Bihlmayer[68] provided band structures for various 1D TM systems which show the effect of turning on spin-orbit coupling and varying the direction of magnetization. Although there is visible shifting and separation of bands, which represent important phenomena in other contexts, these studies show that the effects on both the crossing count and the Fermi-level gradients are fairly minor. There are instances of a change in the number of crossings, such as one additional conduction channel in a Au monowire,[29] and one fewer for a perpendicular magnetization of a Ni monowire,[67] but nothing more significant than this. Therefore, although our band structures should be considered a first approximation, awaiting the inclusion of spin orbit, we maintain that this is unlikely to install a different case from Table I or cause an enormous distortion of Fig. 3. The broad conclusions regarding the computed DSP are probably safe. The omission of the dipolar coupling is justified for similar reasons; indeed, interactions of dipolar origin, on these scales, tend to be significantly weaker even than spin orbit.[55,57,69]

A further caveat is that the spin-orbit coupling may cause spin-flip scattering and thus affect the measured DSP. The likelihood of this declines with increasing spin-diffusion length which in magnetic transition metals can be of the order of 450–1000 Å.[70,71] Moreover, as highlighted in Sec. I, from a theoretical perspective, this would necessitate a more complicated expression for the DSP, rather than—or in addition to—the effects of any minor modification of the band structure itself.

Another potential flaw in our results is the lack of relaxation in the polywire lattice constant.[73] Given that the monowire is the only structure relaxed in this manner, this could be another reason why the DSP in the polywires is immediately so different. However, since the wires become more akin to the three-dimensional crystal with increasing n, the thicker the nanowire, the lower the chances of a dramatic change in lattice constant during relaxation. Therefore, we do not expect a big effect, especially in the thicker wires which still exhibit the interesting DSP discrepancies.

IV. CONCLUSIONS

We focused on three key definitions of the DSP: the DOS or N DSP [Eq. (2)], the ballistic or Nv DSP [Eq. (3)], and the diffusive or Nv^2 DSP [Eq. (4)]. With a detailed examination of a set of feasible nanostructures, we have shown how the commonly used P_N is not necessarily a good indicator of P_{Nv}

or P_{Nv^2}. The paper thus acts as a reminder of the need to choose carefully the definition most relevant for a proposed application or calculates scores under many definitions to maximize the predictive value of the study.

ACKNOWLEDGMENTS

This work was supported by the EPSRC-funded Interdisciplinary Research Collaboration. We thank A. Fisher, D. Pettifor, and A. Ilie for useful discussions.

*ben.hope@cantab.net

†a.horsfield@imperial.ac.uk

[1] G. A. Prinz, Science **282**, 1660 (1998).

[2] S. A. Wolf, D. D. Awschalom, R. A. Buhrman, J. M. Daughton, S. von Molnár, M. L. Roukes, A. Y. Chtchelkanova, and D. M. Treger, Science **294**, 1488 (2001).

[3] I. Žutić, J. Fabian, and S. Das Sarma, Rev. Mod. Phys. **76**, 323 (2004).

[4] S. Das Sarma, Solid State Commun. **119**, 207 (2001).

[5] M. A. Nielsen and I. L. Chuang, *Quantum Computation and Quantum Information* (Cambridge University Press, Cambridge, 2000).

[6] V. V. Zhirnov, R. K. Cavin, J. A. Hutchby, and G. I. Bourianoff, Proc. IEEE **91**, 1934 (2003).

[7] C. You and S. C. Bader, J. Appl. Phys. **87**, 5215 (2000).

[8] A. Ney, C. Pampuch, R. Koch, and K. H. Ploog, Nature (London) **425**, 485 (2003).

[9] W. Wayt Gibbs, Sci. Am. **291**, 57. (2004).

[10] D. C. Worledge and T. H. Geballe, Phys. Rev. Lett. **85**, 5182 (2000).

[11] P. M. Tedrow and R. Meservey, Phys. Rev. Lett. **26**, 192 (1971).

[12] P. M. Tedrow and R. Meservey, Phys. Rev. B **7**, 318 (1973).

[13] R. Meservey and P. M. Tedrow, Phys. Rep. **238**, 173 (1994).

[14] M. Julliere, Phys. Lett. **54A**, 225 (1975).

[15] P. D. Johnson, Rep. Prog. Phys. **60**, 1217 (1997).

[16] A. F. Andreev, Sov. Phys. JETP **19**, 1228 (1964).

[17] C.-K. Yang, J. Zhao, and J. P. Lu, Phys. Rev. Lett. **90**, 257203 (2003).

[18] S. B. Fagan, R. Mota, A. J. R. da Silva, and A. Fazzio, Physica B **340**, 982 (2003).

[19] C.-K. Yang, J. Zhao, and J. P. Lu, Nano Lett. **4**, 561 (2004).

[20] Y. Yagi, T. M. Briere, M. H. F. Sluiter, V. Kumar, A. A. Farajian, and Y. Kawazoe, Phys. Rev. B **69**, 075414 (2004).

[21] S. Dag, E. Durgun, and S. Ciraci, Phys. Rev. B **69**, 121407(R) (2004).

[22] T. Nautiyal, T. H. Rho, and K. S. Kim, Phys. Rev. B **69**, 193404 (2004).

[23] M. Weissmann, G. García, M. Kiwi, and R. Ramírez, Phys. Rev. B **70**, 201401(R) (2004).

[24] H. J. Xiang, J. L. Yang, J. G. Hou, and Q. S. Zhu, New J. Phys. **7**, 39 (2005).

[25] M. Kisaku, M. Rahman, T. Kishi, D. Matsunaka, T. A. Roman, W. A. Diño, H. Nakanishi, and H. Kasai, Jpn. J. Appl. Phys., Part 1 **44**, 882 (2005).

[26] N. Fujima and T. Oda, Phys. Rev. B **71**, 115412 (2005).

[27] M. M. Rahman, M. Kisaku, T. Kishi, T. A. Roman, W. A. Diño, H. Nakanishi, and H. Kasai, J. Phys. Soc. Jpn. **74**, 742 (2005).

[28] Y.-J. Kang, J. Choi, C.-Y. Moon, and K. J. Chang, Phys. Rev. B **71**, 115441 (2005).

[29] Y. Mokrousov, G. Bihlmayer, and S. Blügel, Phys. Rev. B **72**, 045402 (2005).

[30] R. F. Sabirianov, A. K. Solanki, J. D. Burton, S. S. Jaswal, and E. Y. Tsymbal, Phys. Rev. B **72**, 054443 (2005).

[31] M. Weissmann, G. García, M. Kiwi, R. Ramírez, and C. C. Fu, Phys. Rev. B **73**, 125435 (2006).

[32] N. W. Ashcroft and N. D. Mermin, *Solid State Physics* (Holt, Rinehart and Winston, New York, 1976).

[33] I. I. Mazin, Phys. Rev. Lett. **83**, 1427 (1999).

[34] R. Landauer, IBM J. Res. Dev. **1**, 223 (1957).

[35] R. Landauer, Philos. Mag. **21**, 863 (1970).

[36] M. Büttiker, Y. Imry, R. Landauer, and S. Pinhas, Phys. Rev. B **31**, 6207 (1985).

[37] P. B. Allen, Phys. Rev. B **17**, 3725 (1978).

[38] B. Nadgorny, R. J. Soulen, M. S. Osofsky, I. I. Mazin, G. Laprade, R. J. M. van de Veerdonk, A. A. Smits, S. F. Cheng, E. F. Skelton, and S. B. Qadri, Phys. Rev. B **61**, R3788 (2000).

[39] M. S. Osofsky, R. J. Soulen, B. E. Nadgorny, G. Trotter, P. R. Broussard, and W. J. Desisto, Mater. Sci. Eng., B **84**, 49 (2001).

[40] R. P. Panguluri, G. Tsoi, B. Nadgorny, S. H. Chun, N. Samarth, and I. I. Mazin, Phys. Rev. B **68**, 201307(R) (2003).

[41] B. Nadgorny, M. S. Osofsky, D. J. Singh, G. T. Woods, R. J. Soulen, M. K. Lee, S. D. Bu, and C. B. Eom, Appl. Phys. Lett. **82**, 427 (2003).

[42] R. P. Panguluri, C. G. Zeng, H. H. Weitering, J. M. Sullivan, S. C. Erwin, and B. Nadgorny, Phys. Status Solidi B **242**, R67-(2005).

[43] E. Y. Tsymbal and D. G. Pettifor, Phys. Rev. B **54**, 15314 (1996).

[44] R. J. Soulen, J. M. Byers, M. S. Osofsky, B. Nadgorny, T. Ambrose, S. F. Cheng, P. R. Broussard, C. T. Tanaka, J. Nowak, J. S. Moodera *et al.*, Science **282**, 85 (1998).

[45] J. C. Slonczewski, Phys. Rev. B **39**, 6995 (1989).

[46] J. M. MacLaren, X. G. Zhang, and W. H. Butler, Phys. Rev. B **56**, 11827 (1997).

[47] E. Y. Tsymbal and D. G. Pettifor, J. Phys.: Condens. Matter **9**, L411 (1997).

[48] J. Mathon, Phys. Rev. B **56**, 11810 (1997).

[49] J. M. MacLaren, X. G. Zhang, W. H. Butler, and X. D. Wang, Phys. Rev. B **59**, 5470 (1999).

[50] C. Kaiser, A. F. Panchula, and S. S. P. Parkin, Phys. Rev. Lett. **95**, 047202 (2005).

[51] F. Vincent and M. Figlarz, C. R. Seances Acad. Sci., Ser. C **264**, 1270 (1967).

[52] A. Smogunov, A. Dal Corso, and E. Tosatti, Phys. Rev. B **70**, 045417 (2004).

[53] M. Wierzbowska, A. Delin, and E. Tosatti, Phys. Rev. B **72**, 035439 (2005).

[54] A. P. Sutton, *Electronic Structure of Materials* (Oxford University Press, Oxford, 1993).

[55] J. Dorantes-Dávila and G. M. Pastor, Phys. Rev. Lett. **81**, 208

(1998).
[56] M. Komelj, C. Ederer, J. W. Davenport, and M. Fähnle, Phys. Rev. B **66**, 140407(R) (2002).
[57] J. Hong and R. Q. Wu, Phys. Rev. B **67**, 020406(R) (2003).
[58] P. Gambardella, A. Dallmeyer, K. Maiti, M. C. Malagoli, W. Eberhardt, K. Kern, and C. Carbone, Nature (London) **416**, 301 (2002).
[59] V. Rodrigues, J. Bettini, P. C. Silva, and D. Ugarte, Phys. Rev. Lett. **91**, 096801 (2003).
[60] P. Gambardella, J. Phys.: Condens. Matter **15**, S2533 (2003).
[61] P. Gambardella, A. Dallmeyer, K. Maiti, M. C. Malagoli, S. Rusponi, P. Ohresser, W. Eberhardt, C. Carbone, and K. Kern, Phys. Rev. Lett. **93**, 077203 (2004).
[62] S. Dag, S. Tongay, T. Yildirim, E. Durgun, R. T. Senger, C. Y. Fong, and S. Ciraci, Phys. Rev. B **72**, 155444 (2005).
[63] S. Sanvito, *Handbook of Computational Nanotechnolgy* (American Scientific, California, 2004).
[64] G. Tatara, Y. W. Zhao, M. Munoz, and N. Garcia, Phys. Rev. Lett. **83**, 2030 (1999).
[65] H. D. Chopra, M. R. Sullivan, J. N. Armstrong, and S. Z. Hua, Nat. Mater. **4**, 832 (2005).
[66] Y. Mokrousov, G. Bihlmayer, S. Heinze, and S. Blügel, Phys. Rev. Lett. **96**, 147201 (2006).
[67] J. Velev, R. F. Sabirianov, S. S. Jaswal, and E. Y. Tsymbal, Phys. Rev. Lett. **94**, 127203 (2005).
[68] G. Bihlmayer, *Reduced Dimensions II: Magnetic Anisotropy*, Lecture Manuscripts of the Spring School of the Institute of Solid State Research (Forschungszentrum Jülich GmbH, Jülich, 2005), Vol. 36, p. C2.
[69] A. Vindigni, A. Rettori, M. G. Pini, C. Carbone, and P. Gambardella, Appl. Phys. A: Mater. Sci. Process. **82**, 385 (2006).
[70] L. Piraux, S. Dubois, C. Marchal, J. M. Beuken, L. Filipozzi, J. F. Despres, K. Ounadjela, and A. Fert, J. Magn. Magn. Mater. **156**, 317 (1996).
[71] W. C. Chiang, Q. Yang, W. P. Pratt, R. Loloee, and J. Bass, J. Appl. Phys. **81**, 4570 (1997).
[72] The sum is performed over one-half of the first Brillouin zone (BZ1), between the Γ point and an X point, with the sign of the velocity ignored [hence the absolute value of velocity $|v_i|$ being taken in Eq. (3)]. This is due to the symmetry between left- and right-traveling electrons. With zero bias, time reversal symmetry implies that for every left-traveling state, there is a right-travelling state of the same energy (in the opposite half of BZ1). The application of a bias causes more states of one type than the other to be populated, and thus there is a window in which states of only one sign of the velocity are occupied. The magnitude of the current is independent of the sign of the bias (and hence the sign of the velocity) which is why ignoring sign and using only one-half of the zone is sufficient—it gives the same result as counting the number of *populated* channels in the conduction window across the whole zone. The same argument applies to the diffusive polarization definition.
[73] VASP lacks the capacity to relax a cell along one axis only. Achieving this would have involved varying c through manual adjustment of the input, while keeping the two planes separated by $c/2$, and allowing the atoms to relax within the cell at each stage. Performing this for all the wires was unfeasible using the facilities available.